



Title	Temperature dependence of energy gap of (GaAs) <sub>n</sub> /(AlAs) <sub>n</sub> Superlattices
Author(s)	Nakazawa, Takeshi; Matsuoka, Toshimasa; Ohya, Tomoki et al.
Citation	Proceedings of SPIE (1286) : International Conference on Modulation Spectroscopy, 19-21 March 1990, San Diego, California. 1990, p. 244-254
Version Type	VoR
URL	<a href="https://hdl.handle.net/11094/51724">https://hdl.handle.net/11094/51724</a>
rights	Copyright 1990 Society of Photo-Optical Instrumentation Engineers. One print or electronic copy may be made for personal use only. Systematic reproduction and distribution, duplication of any material in this paper for a fee or for commercial purposes, or modification of the content of the paper are prohibited.
Note	

*The University of Osaka Institutional Knowledge Archive : OUKA*

<https://ir.library.osaka-u.ac.jp/>

The University of Osaka

## Temperature dependence of the energy gap of $(\text{GaAs})_n/(\text{AlAs})_n$ superlattices

Takeshi Nakazawa, Toshimasa Matsuoka, Tomoki Ohya, Kenji Taniguchi, Chihiro Hamaguchi

Department of Electronic Engineering,  
Faculty of Engineering, Osaka University, Suita City, Osaka, 565, Japan

Hiroshi Kato and Yasutaka Watanabe

Department of Physics,  
School of Science, Kwansei Gakuin University, Nishinomiya City, Hyogo, 662, Japan

### ABSTRACT

Photoreflectance and photoluminescence experiments are carried out in  $(\text{GaAs})_n/(\text{AlAs})_n$  ( $n = 1-15$ ) in the temperature range from 25 to 275 K. Weak signals of photoreflectance associated with the critical point of the pseudodirect transition, weakly allowed direct transition arising from the zone-folding effect, have been found as well as main signals associated with the direct allowed transitions. This assignment is supported by the temperature dependence of the photoluminescence intensity, which gives the transition probability ratio of the direct allowed to pseudodirect transition about  $10^2$ . Temperature dependence of the critical point energies and luminescence peak energies shows a similar behavior to bulk semiconductors. These observations show also that the monolayer number  $n$  for which the crossover of direct and pseudodirect transitions occurs depends on temperature. In addition the broadening parameters determined from photoreflectance spectra are found to be almost independent of temperature and depend on the monolayer number  $n$ , which may be explained in terms of broadening induced by the layer number fluctuation.

### 1. INTRODUCTION

The development of crystal growth techniques such as molecular beam epitaxy (MBE) has made it possible to produce superlattices (SLs) of high quality. Optical properties of GaAs/AlAs short-period superlattices differ greatly from those of the alloy  $\text{Al}_x\text{Ga}_{1-x}\text{As}$  of equivalent mean composition, showing the importance of the superlattice periodicity in determining the electronic structure of these structures. Some of experimental and theoretical investigations show whether the lowest-energy transition is direct, indirect or so-called pseudodirect and whether it changes as the layer thickness is decreased.<sup>1-10</sup>

In SLs where the coupling through penetrable barriers plays an important role, the miniband is formed because of delocalization of the wave function. From energy band calculations a relative contribution of the atomic states of cations and anions is obtained and it is shown that electronic states of the conduction and valence bands in the unit cell are confined in either GaAs or AlAs layers depending on the monolayer number  $n$ .<sup>8,9</sup> The state confined in GaAs layers is associated with the  $\Gamma$  conduction state of GaAs ( $\Gamma$ -like state), while the latter state with the  $X$  minima of AlAs because the  $X$  minima in AlAs are below those in GaAs due to valence-band offset. Only the  $X_z$  minima are mapped onto  $\Gamma$ -point of the Brillouin zone of the SLs due to the zone-folding effect ( $X_z$ -like state), while the  $X_{xy}$  minima are at  $M$ -point of the Brillouin zone of the SLs ( $X_{xy}$ -like state). Since holes at the  $\Gamma$  maximum of the Brillouin zone of the SLs are confined in GaAs layers, the transition associated with the  $\Gamma$ -like conduction state has large transition probability, while that associated with the  $X_{xy}$ -like and  $X_z$ -like states have small transition probability. Therefore, the  $\Gamma$ -like,  $X_{xy}$ -like and  $X_z$ -like states give the direct and indirect and pseudodirect (weakly allowed direct) transition, respectively. Some of the photoluminescence results are interpreted in terms of spatially indirect transition, where electrons confined in the lowest conduction band at the  $X$ -point of AlAs recombine with holes confined in the valence band at the  $\Gamma$ -point of GaAs.<sup>2</sup>

In our previous work, we reported photoreflectance (PR) and photoluminescence (PL) measurements at room temperature in  $(\text{GaAs})_m/(\text{AlAs})_5$  ( $m = 3-11$ )<sup>11</sup> and  $(\text{GaAs})_n/(\text{AlAs})_n$  ( $n = 1-15$ ) SLs.<sup>12</sup> The experimental results of the former SLs show that the band-crossing occurs at  $m = 7$ , while the latter at  $n = 10$ . This conclusion was drawn from the fact that the observed photoluminescence peaks at lower energy side lie well below the transition energies obtained from PR data and that the transition energy of PR reflects a direct band gap, whereas the lowest PL peaks reflects lower energy band gap, direct or indirect. Theoretical calculations based on the  $sp^3s^*$  tight-binding method<sup>9,10,13</sup> support the experimental observations, where the cross over of the direct and indirect transition occurs at about  $m = 7$  for  $(\text{GaAs})_m/(\text{AlAs})_5$  and at  $n = 10$  for  $(\text{GaAs})_n/(\text{AlAs})_n$ . In our previous paper<sup>12</sup> we observed a weak structure below the strong structure in  $(\text{GaAs})_5/(\text{AlAs})_5$ , where the transition energy of the weak structure corresponds to the photoluminescence peak at low energy side. This result may be interpreted in terms that the weak structure arises from the zone-folding effect, that is, transition between the zone-folded  $X_z$ -like conduction band and the top valence band at the  $\Gamma$ -point. This weak structure on PR was observed only in  $(\text{GaAs})_5/(\text{AlAs})_5$  and thus we assigned the weak structure not to the pseudodirect transition but the indirect transition. As reported in our paper to be presented at this conference,<sup>14</sup> we observed the weak structure in  $(\text{GaAs})_n/(\text{AlAs})_n$  with  $n \leq 12$ , and thus we conclude that the weak structure in PR arises from the pseudodirect (weakly allowed direct) transition.

It is expected that the band crossing depends on temperature because the band gaps of bulk semiconductors vary as the temperature is changed and the temperature dependence of the direct gap and indirect gap is different. Kato *et al.*<sup>6</sup> reported photoluminescence measurements at low temperatures and they found that the band crossing occurs at  $n = 14$  in  $(\text{GaAs})_n/(\text{AlAs})_n$ . As stated above our measurements at room temperature show the band crossing at around  $n = 10$ . These results indicate that the band crossing depends on temperature.

In this paper, we discuss the temperature dependence of the energy band gaps of the  $(\text{GaAs})_n/(\text{AlAs})_n$  ( $n = 1-15$ ) SLs, placing our main emphasis on the temperature dependence of the band crossing in addition to the origin of the weak structure in PR at low energy side. Experiments were carried out in the temperature range from 25 to 275 K. We estimated the ratio of the transition probability between the weakly allowed (pseudodirect) and allowed direct transition, and the ratio was found to be about  $10^{-2}$  from the experimental results PL.

## 2. EXPERIMENTAL

The set of  $(\text{GaAs})_n/(\text{AlAs})_n$  samples used in this work were epitaxially grown at 570 °C on (100) semi-insulating GaAs substrates by MBE. The values of atomic layer number  $n$  were 1-15 and the multiple layers were about 200 periods. The number of GaAs and AlAs layers was accurately controlled by counting the period of the intensity oscillations of a specularly reflected beam in a reflection high energy electron diffraction (RHEED) pattern.<sup>15</sup> The thickness of the individual atomic layer of the SLs has been measured using x-ray diffraction method,<sup>16</sup> and the SLs were found to be good in quality.

The PR experimental arrangement used in the present work is similar to that used by Glembocki *et al.*<sup>17</sup> and Shay,<sup>18</sup> as shown schematically in Fig. 1. A monochromatic probe light and a pumping laser beam are incident on the same spot of the sample surface, and a reflected probe light through a filter blocking the laser light is focused onto a photomultiplier tube (PMT) to observe the reflectivity change caused by the pumping laser beam chopped mechanically. Signals from the PMT are amplified by a lock-in-amplifier tuned to the modulation frequency of the chopper. An electric servo mechanism on the high-voltage power supply of the PMT is used to maintain a constant DC voltage across the load resistance of the PMT, allowing us to obtain the ratio  $\Delta R/R$  directly. We used a 500 W Xe arc lamp for the probe light source and a 50cm single monochromator of JASCO CT-50S with a 1200 lines/mm grating blazed at 750 nm. The intensity of the Ar ion laser light (488.0 nm) chopped at 210 Hz for modulation was reduced to about 0.5 mW by using neutral density filters. For PL measurements, the

sample were excited with about 10 mW of the Ar ion laser light (488.0 or 476.5 nm) and luminescence spectra were measured with an 80 cm focal length double monochromator (Spex 1401). The temperature of the sample is controlled by a Helium-closed-cycle refrigerator in the range from 25 to 300 K. The digitized data of optical signals and temperature are recorded by a personal computer and transferred into a computer (HP9000 Model 550) for detailed analysis.

The experimental data of PR are analyzed using the third-derivative formula derived by Aspnes.<sup>19,20</sup>, which is given by

$$\frac{\Delta R}{R} = \sum_j^p \text{Re}[C_j \exp(i\theta_j)(E - E_{gj} + i\Gamma_j)^{-m_j}], \quad (1)$$

where  $p$  is the number of critical points,  $E$  the photon energy,  $C_j$ ,  $\theta_j$ ,  $E_{gj}$  and  $\Gamma_j$  are the amplitude, phase, energy gap, broadening parameter, respectively, of the  $j$ -th critical point. The value of  $m_j$  is a parameter which depends on the critical point type,  $m_j = 3.5$ , 3.0 and 2.5 for the one-, two-, and three-dimensional critical point, respectively. As the electrons and holes are extended in the SLs, we use  $m_j = 2.5$  (three-dimensional critical point). The values of the parameters stated above are evaluated by fitting the line shape of the third-derivative formula to the experimental data of PR, based on the method proposed by Rosenbrock.<sup>21</sup> Details of the reflectance analysis are given elsewhere.<sup>11,12,14</sup>

### 3. RESULTS AND DISCUSSION

Figure 2(a), 2(b) and 2(c) show the PR and PL spectra of the  $(\text{GaAs})_{13}/(\text{AlAs})_{13}$  at 250 K, 150 K and 50 K, respectively, together with the fitted PR spectra, where the arrows show the critical point energies obtained by the fitting procedure. The PL spectra at 150 K and 250 K consist of a main peak at

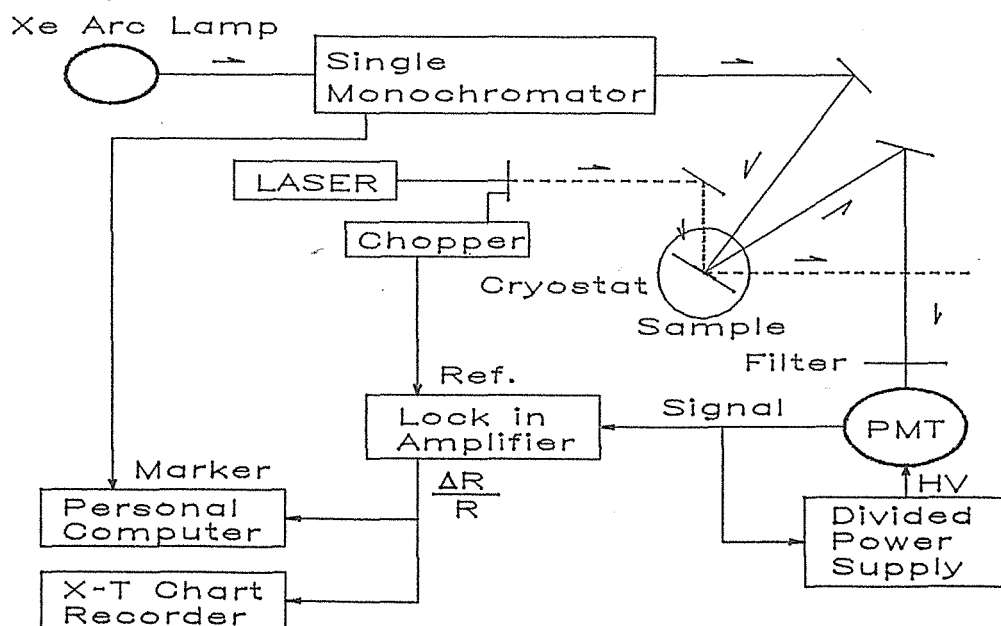


Fig. 1. Schematic diagram of the photorefectance setup used in the present work. The laser beam from an Ar ion laser is chopped at a frequency of 210 Hz. Signals are detected by a photomultiplier tube and amplified by a lock-in-amplifier and recorded by a personal computer. The sample temperature is controlled by a cryostat.

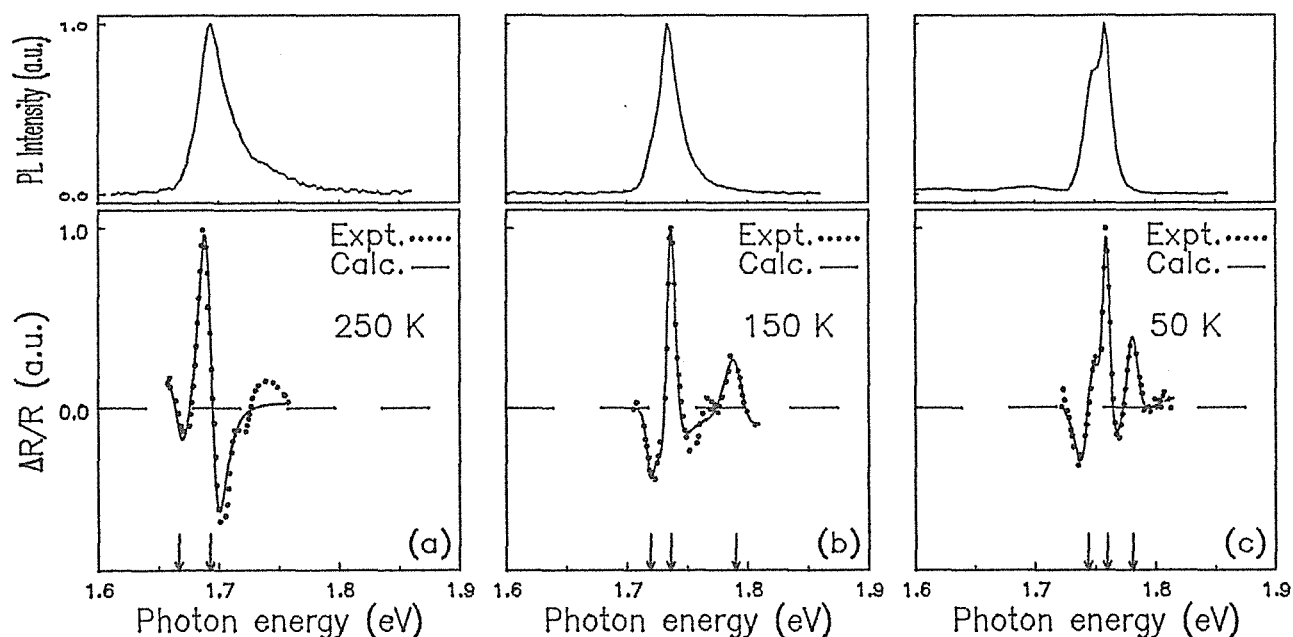


Fig. 2. Experimental spectra of PR (lower trace) and PL (upper trace) for the  $(\text{GaAs})_{13}/(\text{AlAs})_{13}$  SL sample (a) at 250 K, (b) at 150 K and (c) at 50 K are shown, where the solid curve represent the best fitted curve by using the third-derivative formula given in the text. The vertical arrows indicate the critical point energies obtained by the fitting best fitting.

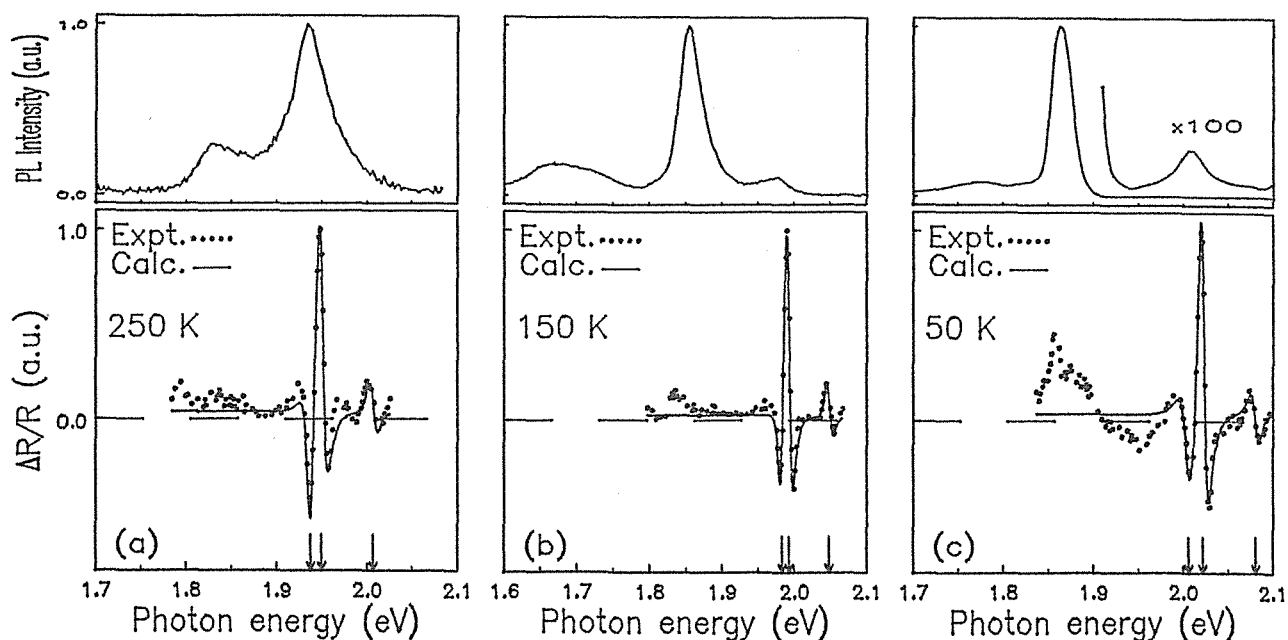


Fig. 3. PR and PL spectra for the  $(\text{GaAs})_7/(\text{AlAs})_7$  SL sample (a) at 250 K, (b) at 150 K and (c) at 50 K, where the upper and lower curves represent PL and PR spectra, respectively. The solid curve in PR spectra is obtained from the best fitting and the vertical arrows indicate the critical point energies determined by the fitting.

1.733 eV and 1.693 eV, respectively, whereas we observe that the peak splits into two peaks at 1.746 eV and 1.758 eV at 50 K. The observed PR spectra at 250 K are resolved into two structures of which critical point energies are 1.667 eV and 1.693 eV, respectively, and the critical point energy of the main structure in PR corresponds to the PL peak energy. In Fig. 2(a) the PL spectra have shoulders at lower and higher energy sides, which are not well resolved. The PR spectra shown in Fig. 2(a) may be resolved into three structures and the weak structures at the lower and higher energy side of the main structure seem to correspond to the shoulders in the PL. In the present analysis, however, we performed best fitting by using two critical point energies, neglecting the structure in the higher energy region, and thus we obtained two critical points indicated by the arrows. At 150 K the PR spectra are resolved into three structures and the corresponding transition energies are, 1.719 eV, 1.736 eV and 1.790 eV, where we find that the critical point energy 1.736 eV of the main structure agrees well with the PL peak energy. At 50 K the PR data are resolved into three structures and the corresponding critical point energies are 1.744 eV, 1.760 eV, and 1.781 eV, and the lower two energies are in good agreement with the lower two peak energies of the PL data at 1.746 eV and 1.758 eV.

Since PR signals are induced by direct transition process, the observed PL peaks are ascribed to the direct transition. The reason why the higher energy transition was not observed in PL experiments is as the following. The emission intensity of PL depends on the magnitude of the transition probability and also the absorption coefficient. Emission at higher energy side becomes weaker due to stronger absorption, and therefore only two peaks are observed in PL spectra. The photon energies obtained from the present analysis of PR are in the range from 1.6 to 1.8 eV, and thus the transition is ascribed to direct band gap at the  $\Gamma$ -point. Due to the zone-folding effect, there exist many conduction bands at the  $\Gamma$ -point in a narrow range of energy, and thus we can expect many critical points. However, we have to note that the optical transition depends on the joint density of states and also momentum matrix elements, which are determined by the energy bands, dispersion of the bands and wave functions. In Fig. 2 we find that the critical point energies, band gaps, increase as the temperature is decreased.

Similar results for  $(\text{GaAs})_7/(\text{AlAs})_7$  are presented in Fig. 3(a) at 250 K, 3(b) at 150 K, and 3(c) at 50 K, where the upper trace shows PL data and the lower curves show PR data and best fitted curve. The

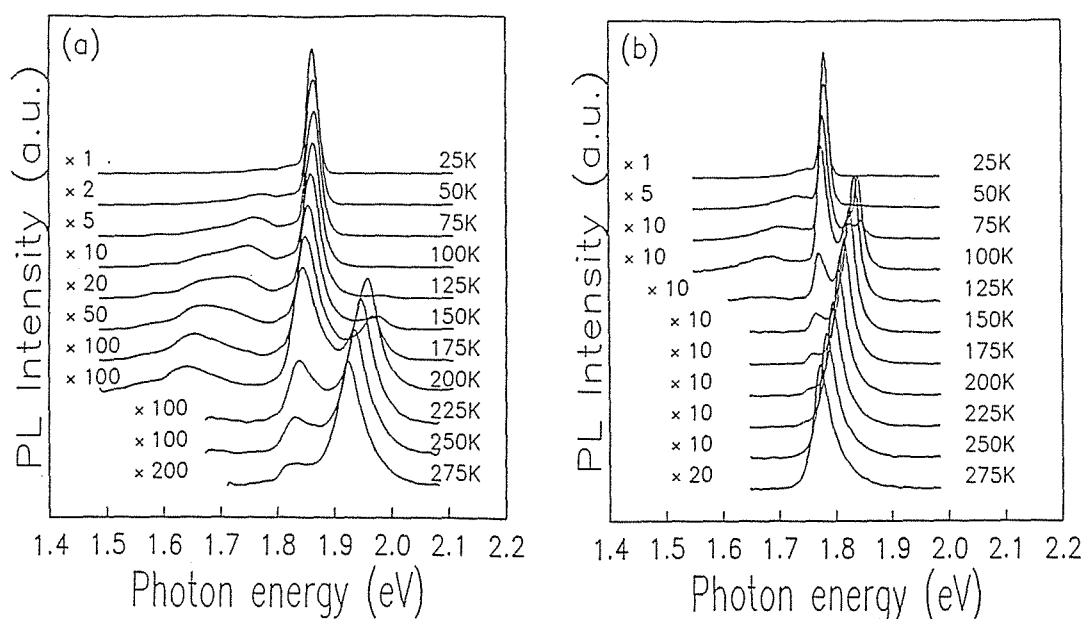


Fig. 4. PL spectra of (a) the  $(\text{GaAs})_7/(\text{AlAs})_7$  and (b) the  $(\text{GaAs})_{10}/(\text{AlAs})_{10}$  are plotted at various temperatures (from 25 K to 275 K) for comparison in the photon energy region where emissions of the pseudodirect and direct transitions appear.

best fitting of the PR spectra gives transition energies 1.938 eV, 1.950 eV, and 2.009 eV at 250 K, 1.983 eV, 1.993 eV and 2.048 eV at 150 K, and 2.006 eV, 2.024 eV and 2.079 eV at 50 K. In PR spectra shown in Fig. 3 we see well separated weak structure at lower energy side, where the PR structure at the lower energy side is not analyzed by best fitting because of low quality of data, but the structure is reproducibly observed and the signals exceed the range of experimental error. The spectra of PL for (GaAs)<sub>7</sub>/(AlAs)<sub>7</sub> are quite different from those for (GaAs)<sub>13</sub>/(AlAs)<sub>13</sub>, where the low energy peak of PL which corresponds to the weak structure of PR at lower energy side, is much stronger than the higher energy peak. As in the case of (GaAs)<sub>13</sub>/(AlAs)<sub>13</sub>, only one main peak is observed in PL, while three critical points are resolved in the PR spectra in the same photon energy region. We find in Fig. 3(b) a weak and broad emission is observed in PL at about 1.70 eV, where we see no structure in PR. In the present work we found that the low energy emission appears at some range of lattice temperature.<sup>14</sup>

The emission at the higher energy side appears in the photon energy region where the main structure of PR is observed (two vertical arrows at lower energy side in Fig. 3). The PL peak, 2.006 eV at 50 K, 1.979 eV at 150 K and 1.934 eV at 250 K, respectively, is in good agreement with the transition energy of PR main signals at 2.006 eV at 50 K, 1.983 eV at 150 K and 1.938 eV at 250 K. This structure is assigned as the allowed direct transition at the  $\Gamma$ -point. The weak structure of PR signals in the photon energy region from 1.8 to 1.9 eV, well below the main structure of PR, corresponds to the PL emission band at 1.862 eV at 50 K, 1.855 eV at 150 K, and 1.830 eV at 250 K. The weak structure of PR at lower energy side may be interpreted in terms of pseudodirect transition (weakly allowed direct transition) arising from the zone-folding effect. This assignment is supported by a comparison with the energy band calculations based on the tight-binding method<sup>14</sup> and also by the analysis shown below.

The temperature dependence of the PL spectra for (GaAs)<sub>7</sub>/(AlAs)<sub>7</sub> is shown in Fig. 4 (a). Based on the discussion stated above, the higher- and lower-energy peaks are assigned to be the direct and pseudodirect, respectively. Figure 4 (b) shows the temperature dependence of the PL spectra for (GaAs)<sub>10</sub>/(AlAs)<sub>10</sub>, in which the assignment of the two peaks is the same as those in Fig. 4 (a), direct and pseudodirect transitions. In Figs. 4 (a) and (b) intensity of the PL peak at higher energy side decreases and the other

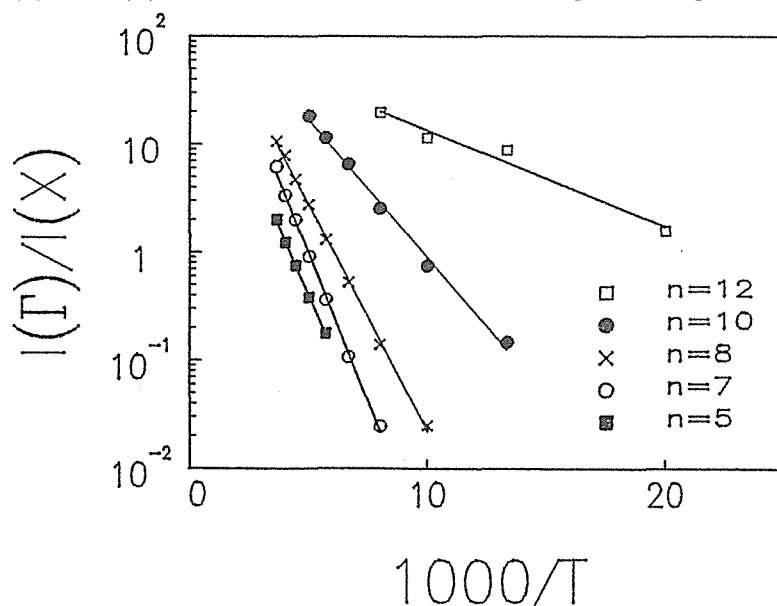


Fig. 5. The ratio of the PL peak intensity of the direct transition to the pseudodirect transition is plotted as a function of inverse temperature for the (GaAs)<sub>n</sub>/(AlAs)<sub>n</sub> SLs with  $n = 5, 7, 8, 10$ , and  $12$ , where the slope gives the energy separation and the intercept of the curve at zero gives the ration of the transition probabilities (see text in detail).

peak at lower energy side increases as the temperature decreases. It is very important to point out that the temperature at which the intensity of the two peaks becomes equal is higher for  $(\text{GaAs})_n/(\text{AlAs})_n$  with smaller  $n$ . This feature indicates that the separation of the energy gaps between the pseudodirect and direct band gaps increases with decreasing the monolayer number  $n$ .

Intensity of emission depends on the transition probability and number of carriers excited. In the following we assume the emission is governed by the two factors and neglect the effect of absorption. With this approximation we are able to estimate the transition probability and the energy separation from the data shown in Figs. 4 (a) and (b). Under this assumption the PL intensity is proportional to the product of electron density at the conduction band and the transition probability, and the ratio of the PL emission between the direct gap ( $E_\Gamma$ ) and the pseudodirect band gap ( $E_X$ ) is written as

$$\frac{I(\Gamma)}{I(X)} = \frac{W_\Gamma}{W_X} \exp\left(\frac{E_X - E_\Gamma}{k_B T}\right), \quad (2)$$

where  $I(\Gamma)$ ,  $E_\Gamma$  and  $W_\Gamma$  are PL intensity, transition energy and transition probability for the direct allowed transition (wave function of the conduction band has predominantly the character of the  $\Gamma$  band of GaAs), and  $I(X)$ ,  $E_X$  and  $W_X$  for the pseudodirect transition (wave function of the conduction band has predominantly the character of the  $X$  band of AlAs, and referred to as  $X_z$ -like state in this paper),  $k_B$  is the Boltzmann constant. In eq.(2) the factor of the effective mass or the density of states is ignored, but we have to remind that the effective mass of the  $X_z$ -like band is very heavy as seen in the energy band calculations.<sup>12</sup>

Figure 5 shows the intensity ratio  $I(\Gamma)/I(X)$  as a function of inverse temperature obtained from the present experiments shown in Figs. 4 (a) and (b) together with the least square fit lines. These lines for  $(\text{GaAs})_n/(\text{AlAs})_n$  with  $n = 5, 7, 8, 10$ , and  $12$  give the energy separation  $E_\Gamma - E_X = 100$  meV, 109 meV,

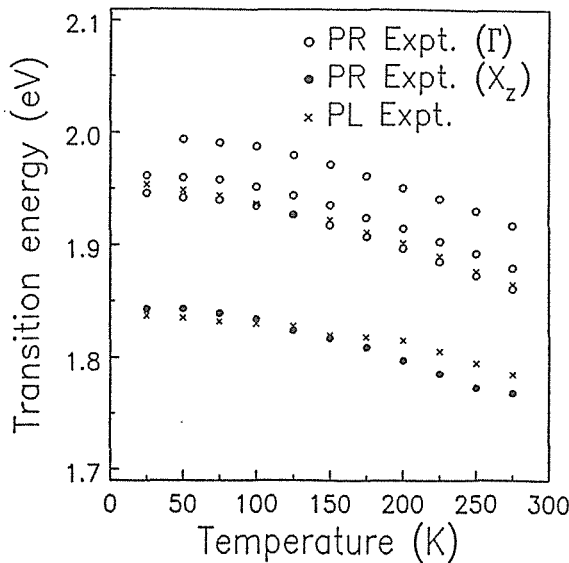


Fig. 6. Temperature dependence of the transition energies obtained by PR and PL measurements in the  $(\text{GaAs})_8/(\text{AlAs})_8$  SL, where the open (higher transition energies, allowed direct) and solid circles (lower transition energies, pseudodirect) are the energies determined from the PR and the crosses are PL peak energies.

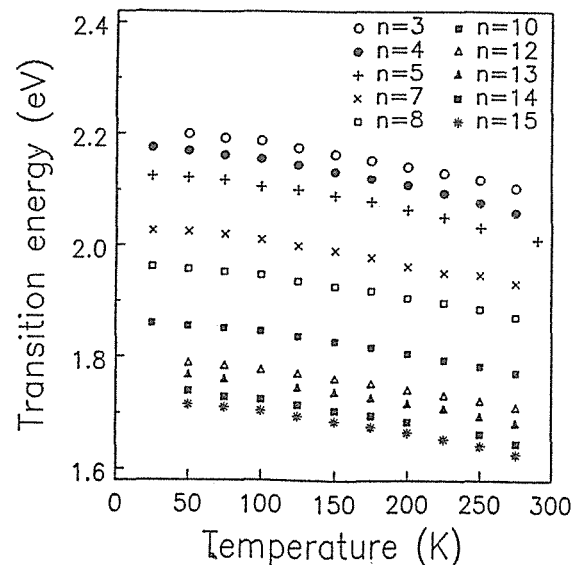


Fig. 7. Temperature dependence of the lowest direct allowed transition energy obtained by PR measurement are plotted as a function of temperature in the  $(\text{GaAs})_n/(\text{AlAs})_n$  SLs with  $n = 3, 4, 5, 7, 8, 10, 12, 13, 14$ , and  $15$  from the top to the bottom.



83 meV, 50 meV, and 18 meV, respectively. From the intercept of the line the ratio of transition probabilities  $W_X/W_\Gamma$  is estimated to be  $7.7 \times 10^{-3}$ ,  $1.8 \times 10^{-3}$ ,  $2.9 \times 10^{-3}$ ,  $3.1 \times 10^{-3}$ , and  $6.9 \times 10^{-3}$  for  $n = 5, 7, 8, 10$ , and  $12$ , respectively. The energy separation is in reasonable agreement with the transition energy obtained earlier (within about 10 % difference except  $(\text{GaAs})_{12}/(\text{AlAs})_{12}$ ). In addition the ratio of the transition probability suggests that the transition at the lower energy side is much weaker (by two or three orders of magnitude, or more if we take into account the difference in the effective mass). Therefore, these results strongly suggest that the lower-energy band gap is ascribed to a pseudodirect band gap at the  $\Gamma$ -point, resulting from the zone-folding and thus electronic state is associated with the  $X_z$ -like state. The ratio of the transition probability obtained in the present work is consistent with the ratio of photoluminescence decay time between the two emission bands.<sup>1,6,22,23</sup>

Figure 6 shows temperature dependence of the transition energies in  $(\text{GaAs})_8/(\text{AlAs})_8$  SL, where transition energies determined from the PR and PL are plotted by the circles (open and solid circles) and crosses, respectively. We find in Fig. 6 that the three transition energies obtained from the PR analysis decrease monotonously with increasing temperature and the shift is about 100 meV in the temperature range from 25 to 300 K, while the PL peaks at the lower energy side, ascribed to the pseudodirect transition, exhibits about 70 meV shift in the same temperature range. The energy shift of the transition energies determined from the PR experiments is quite similar to that of the fundamental energy gap of bulk GaAs. We find in Fig. 6 that the transition energy of the PR main structure agrees well with the PL peak at the higher energy side in the temperature range. On the other hand, there exists a slight difference in the temperature dependence between the lowest transition energy determined from PR analysis and the low-energy side peak of PL, and the shift of the PL peak energy is smaller. The difference is higher at higher temperatures and about 20 meV at 250 K. We assigned this transition as the pseudodirect transition due to the zone-folding effect and thus the transition energy is expected to agree with each other within the range of phonon energy. Crossing of the transition energies at about 120 K is not understood at the present stage.

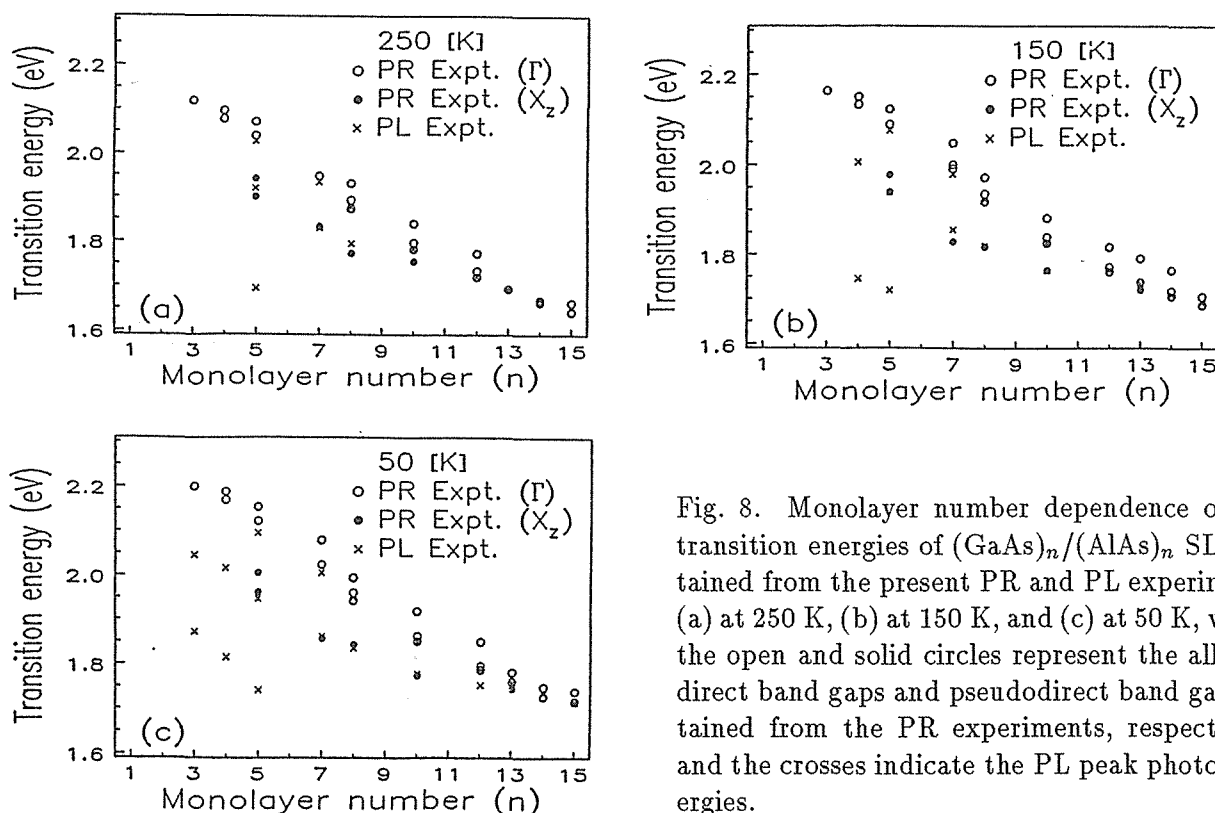


Fig. 8. Monolayer number dependence of the transition energies of  $(\text{GaAs})_n/(\text{AlAs})_n$  SLs obtained from the present PR and PL experiments (a) at 250 K, (b) at 150 K, and (c) at 50 K, where the open and solid circles represent the allowed direct band gaps and pseudodirect band gap obtained from the PR experiments, respectively, and the crosses indicate the PL peak photon energies.

Similar behavior is observed in other  $(\text{GaAs})_n/(\text{AlAs})_n$ . In Fig. 7 we plot only the transition energy corresponding to the main structure of the PR signals as a function of temperature for  $(\text{GaAs})_n/(\text{AlAs})_n$  with  $n = 3$  to 15. All the samples exhibit a quite similar feature in their temperature dependence. Taking into account the fact that the conduction band associated with this transition reflects the nature of the conduction band of GaAs at the  $\Gamma$  point, its temperature dependence is expected to be similar to that of GaAs.

In Fig. 8 (a), (b) and (c) we plot the monolayer number ( $n$ ) dependence of the transition energies determined from the PR and PL measurements at 50 K, 150 K and 250 K, respectively, in  $(\text{GaAs})_n/(\text{AlAs})_n$  with  $n = 1$ -15, where the open and solid circles (notation PR Expt. ( $\Gamma$ )) represent transition energies determined from the PR analysis, and the crosses are the PL peak energies. The notation ( $\Gamma$ ) and ( $X_z$ ) is used from the reason stated earlier, where the upper transition energies determined from the PR is understood to be due to the allowed direct transition at the  $\Gamma$  point and the lower weak structure of the PR arises from the pseudodirect transition (the zone-folded conduction band with the wave function of the  $X$  state of AlAs). The pseudodirect transition appears at 50 K in  $(\text{GaAs})_n/(\text{AlAs})_n$  with  $n < 14$ , and at 150 K and 250 K in  $(\text{GaAs})_n/(\text{AlAs})_n$  with  $n < 11$ . This suggests that the direct-pseudodirect crossover depends on temperature and at lower temperatures the crossover occurs in  $(\text{GaAs})_n/(\text{AlAs})_n$  with larger  $n$ . This temperature dependence of the crossover will explain the difference between our previous work<sup>12</sup> and the work by Kato *et al.*<sup>6</sup> One of the most probable possibilities for this temperature dependence may be the difference in the temperature dependence of the energy gaps of GaAs and AlAs, where the temperature dependence of the gap in AlAs is slightly smaller than that of GaAs. Noting that the pseudodirect gap reflects the nature of the conduction band at the  $X$ -point of AlAs, its temperature dependence is expected weaker compared to that of the allowed direct band gap. In Fig. 6 we found that the pseudodirect gap obtained from the PR experiments behaves quite similarly to that of the direct gap of GaAs, although the gap determined from the PL data behaves similarly to that of indirect band gap of AlAs. However, some of the  $(\text{GaAs})_n/(\text{AlAs})_n$  with small  $n$  exhibit difference in the temperature dependence between the pseudodirect and allowed direct gaps. It should be noted that the weak structure in PR spectra depends strongly on the temperature.

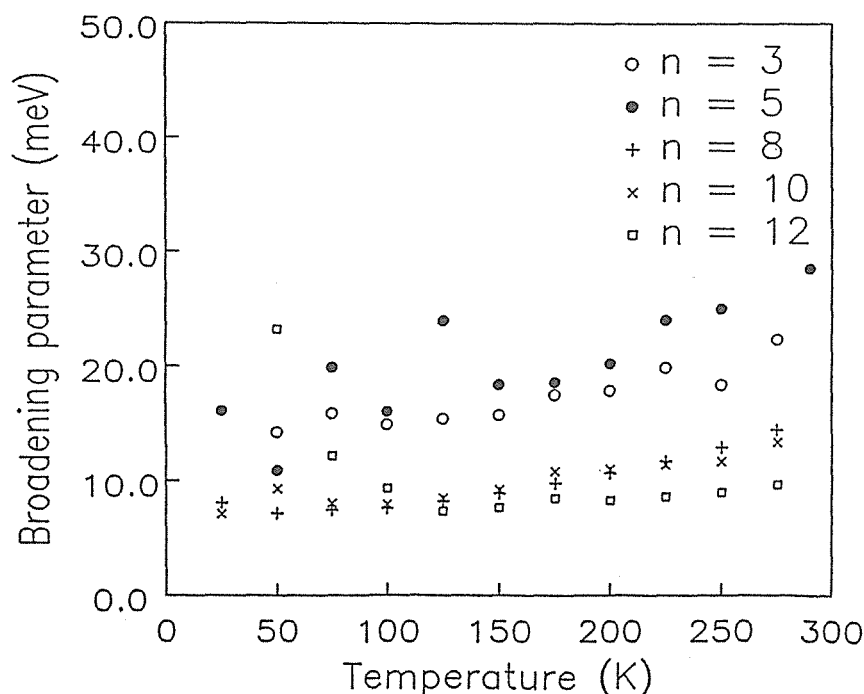


Fig. 9. Temperature dependence of the broadening parameter of PR spectra for  $(\text{GaAs})_n/(\text{AlAs})_n$  SLs with  $n = 3, 5, 8, 10$ , and 12, where the broadening parameter for the lowest direct gap is plotted.

In Fig. 8 we find PL peak energies, in the photon energy region around 1.7 to 1.75 eV, which are well below the pseudodirect gap and seen in Fig. 2(c). The energy is higher than the band gap of GaAs and thus the PL signals are not ascribed to the emission from the substrate. If this emission band arise from the superlattice layers, the signals are assigned to the transition from the conduction band associated with the  $X_{xy}$ -like state to the top valence band at the  $\Gamma$ -point, because the  $X_{xy}$ -like state is expected to be lower than the  $X_z$ -like state for small  $n$ . This band alignment is shown by the tight-binding calculation.<sup>10</sup>

The analysis of PR spectra using the third-derivative formula<sup>19,20</sup> gives the broadening parameter for each critical point. Temperature dependence of the broadening parameter of the main PR signals (lower critical point for the allowed direct transition) for  $(\text{GaAs})_n/(\text{AlAs})_n$  with  $n = 3, 5, 8, 10$ , and 12 are shown in Fig. 9. These broadening parameters are almost independent of the temperature but depend on the monolayer number  $n$ . The broadening parameters decrease with increasing  $n$ , except  $(\text{GaAs})_5/(\text{AlAs})_5$ . Since the broadening parameters are almost independent of the temperature, the broadening arises not from the electron-phonon interactions but from other effects. We pointed out in our previous paper<sup>12</sup> that the broadening is induced by the fluctuation of monolayers during the growth of the SLs. Although the monolayer number was carefully controlled by observing RHEED oscillations, it is very difficult to obtain uniform periodicity of the monolayer number in the whole region of the samples used in the PR measurements. This layer number fluctuation also results in a considerable change in the energy gaps as shown in our paper<sup>14</sup>, where we calculated energy band structures of a long period superlattice such as  $(\text{GaAs})_n/(\text{AlAs})_n/(\text{GaAs})_{n+1}/(\text{AlAs})_n$  and the lowest direct gap is about 100 meV lower than  $(\text{GaAs})_n/(\text{AlAs})_n$  for  $n = 4$ .

#### 4. CONCLUSIONS

Photoreflectance and photoluminescence measurements have been carried out in short period superlattices  $(\text{GaAs})_n/(\text{AlAs})_n$  with  $n = 1-15$ , placing main emphasis on the temperature dependence of the band gaps. We observed a weak structure in PR spectra well below the main structure in  $(\text{GaAs})_n/(\text{AlAs})_n$  with  $n$  less than about 13. The weak structure was ascribed to the pseudodirect transition between the zone-folded conduction band (the wave function of  $X_z$ -like) and the valence band at the  $\Gamma$ -point. The main structure is interpreted in terms of the allowed direct transition between the conduction band (the wave function of  $\Gamma$  state of GaAs) and the valence band at the  $\Gamma$ -point. The weak structure was observed in  $(\text{GaAs})_n/(\text{AlAs})_n$  with  $n = 5, 7, 8, 10$ , and 13, and the intensity of the signals depends on temperature. Since the PR signals arise from direct transition, we ascribed this weak structure as arising from the pseudodirect transition. Temperature dependence of the PL intensity ratio between the direct allowed and pseudodirect transitions has revealed that the transition probability of the pseudodirect transition is smaller by two orders of magnitude than that of the direct transition. Transition energies determined from the PR measurements show a similar behavior to the that of the fundamental absorption edge of GaAs, whereas the photoluminescence peak corresponding to the pseudodirect transition shows slightly weaker temperature dependence. Our observations show that the direct-pseudodirect crossover in  $(\text{GaAs})_n/(\text{AlAs})_n$  occurs for  $n = 14$  at 50 K and for  $n = 11$  at 150 K and 250 K. The analysis of PR spectra also reveals that the broadening is caused by the lateral fluctuation of the superlattices.

#### 5. REFERENCES

- <sup>1</sup>E. Finkman, M. D. Sturge and M. C. Tamargo, "X-point Excitons in AlAs/GaAs Superlattices," Appl. Phys. Lett. **49**, pp. 1299-1301, November 1986.
- <sup>2</sup>D. S. Jiang, K. Kelting, H. J. Queisser and K. Ploog, "Luminescence Properties of  $(\text{GaAs})_l/(\text{AlAs})_m$  Superlattices with  $(l,m)$  Ranging from 1 to 73," J. Appl. Phys. **63**, pp. 845-852, February 1988.
- <sup>3</sup>M. Recio, J. L. Castano and F. Briones, "Optical Properties of GaAs/AlAs Short Period Superlattices," Jpn. J. Appl. Phys. **27**, pp. 1204-1209, July 1988.

- <sup>4</sup>K. J. Moore, P. Dawson and C. T. Foxon, "Effects of Electronic Coupling on the Band Alignment of Thin GaAs/AlAs Quantum-well Structures," *Phys. Rev. B* **38**, pp. 3368-3374, August 1988.
- <sup>5</sup>K. J. Moore, G. Duggan, P. Dawson and C. T. Foxon, "Short-period GaAs-AlAs Superlattices: Optical Properties and Electronic Structure," *Phys. Rev. B* **38**, pp. 5535-5542, September 1988.
- <sup>6</sup>H. Kato, Y. Okada, M. Nakayama and Y. Watanabe, "T-X Crossover in GaAs/AlAs Superlattices," *Solid State Commun.* **70**, pp. 535-539, 1989.
- <sup>7</sup>M. Nakayama, I. Tanaka, I. Kimura and H. Nishimura, "Photoluminescence Properties of GaAs/AlAs Short-Period Superlattices," *Jpn. J. Appl. Phys.* **29**, pp. 41-47, January 1990.
- <sup>8</sup>J. N. Schulman and T. C. McGill, "Electronic Properties of the AlAs-GaAs (001) Interface and Superlattice," *Phys. Rev. B* **19**, pp. 6341-6349, June 1979.
- <sup>9</sup>E. Yamaguchi, "Theory of the DX Centers in III-V Semiconductors and (001) Superlattices," *J. Phys. Soc. Jpn.* **56**, pp. 2835-2852, August 1987.
- <sup>10</sup>J. Ihm, "Effects of the Layer Thickness on the Electronic Character in GaAs-AlAs Superlattices," *Appl. Phys. Lett.* **50**, pp. 1068-1070, April 1987.
- <sup>11</sup>T. Nakazawa, H. Fujimoto, K. Imanishi, K. Taniguchi, C. Hamaguchi, S. Hiyamizu and S. Sasa, "Photorefectance and Photoluminescence Study of  $(\text{GaAs})_m/(\text{AlAs})_5$  ( $m = 3-11$ ) Superlattices: Direct and Indirect Transition," *J. Phys. Soc. Jpn.* **58**, pp. 2192-2199, June 1989.
- <sup>12</sup>H. Fujimoto, C. Hamaguchi, T. Nakazawa, K. Taniguchi, K. Imanishi, H. Kato and Y. Watanabe, "Direct and Indirect Transition in  $(\text{GaAs})_n/(\text{AlAs})_n$  Superlattices with  $n = 1-15$ ," *Phys. Rev. B* **41**, April 1990 (to be published).
- <sup>13</sup>P. Vogl, H. P. Hjalmarson and J. D. Dow, "A Semi-empirical Tight-binding Theory of the Electronic Structure of Semiconductors," *J. Phys. Chem. Solids* **44**, pp. 365-378, 1983.
- <sup>14</sup>C. Hamaguchi, T. Nakazawa, T. Matsuoka, T. Ohya, K. Taniguchi, H. Fujimoto, K. Imanishi, H. Kato and Y. Watanabe, "Direct and Indirect Transition in  $(\text{GaAs})_n/(\text{AlAs})_n$  Superlattices with  $n = 1-15$ ," *SPIE Int. Conf. on Modulation Spectroscopy*, San Diego, March 19-21, 1990, in this proceedings.
- <sup>15</sup>N. Sano, H. Kato, M. Nakayama, S. Chika and H. Terauchi, "Mono- and Bi-Layer Superlattices of GaAs and AlAs," *Jpn. J. Appl. Phys.* **23**, pp. L640-L641, August 1984.
- <sup>16</sup>H. Terauchi, Y. Noda, K. Kamigaki, S. Matsunaka, M. Nakayama, H. Kato, N. Sano and Y. Yamada, "X-Ray Diffraction Patterns of Configurational Fibonacci Lattices," *J. Phys. Soc. Jpn.* **57**, pp. 2416-2424, July 1988.
- <sup>17</sup>O. J. Glembocki, B. J. Shanabrook, N. Bottka, W. T. Beard and J. Comas, "Photorefectance Characterization of Interband Transition in GaAs/AlGaAs Multiple Quantum Wells and Modulation-doped Heterojunctions," *Appl. Phys. Lett.* **46**, pp. 970-972, May 1985.
- <sup>18</sup>J. L. Shay, "Photorefectance Line Shape at the Fundamental Edge in Ultrapure GaAs," *Phys. Rev. B* **2**, pp. 803-807, August 1970.
- <sup>19</sup>D. E. Aspnes and J. E. Rowe, "Resonant Nonlinear Optical Susceptibility: Electroreflectance in the Low-Field Limit," *Phys. Rev. B* **5**, pp. 4022-4030, May 1972.
- <sup>20</sup>D. E. Aspnes, "Third-derivative Modulation Spectroscopy with Low-field Electroreflectance," *Surf. Sci.* **37**, pp. 418-442, 1973.
- <sup>21</sup>H. H. Rosenbrock, "An Automatic Method for Finding the Greatest or Least Value of a Function," *The Computer Journal* **3**, pp. 175-184, 1960.
- <sup>22</sup>J. Feldmann, G. Peter, E. O. Gobel, P. Dawson, K. Moore, C. Foxon and R. J. Elliott, "Linewidth Dependence of Radiative Exciton Lifetimes in Quantum Wells," *Phys. Rev. Lett.* **59**, pp. 2337-2340, November 1987.
- <sup>23</sup>F. Minami, K. Hirata, K. Era, T. Yao and Y. Masumoto, "Localized Indirect Excitons in a Short-period GaAs/AlAs Superlattices," *Phys. Rev. B* **36**, pp. 2875-2878, August 1987.